Ultrasound in Med. & Biol., Vol. 31, No. 10, pp. 1383–1389, 2005
Copyright © 2005 World Federation for Ultrasound in Medicine & Biology
Printed in the USA. All rights reserved
0301-5629/05/$–see front matter

ELSEVIER

doi:10.1016/j.ultrasmedbio.2005.06.004

● *Original Contribution*

GEL PHANTOM FOR USE IN HIGH-INTENSITY FOCUSED ULTRASOUND DOSIMETRY

Cyril Lafon,* Vesna Zderic,† Misty L. Noble,‡ Jonathan C. Yuen,‡ Peter J. Kaczkowski,† Oleg A. Sapozhnikov,†§ Francoise Chavrier,* Lawrence A. Crum,†‡ and Shahram Vaezy†‡

*Inserm, Lyon, France; †Center for Industrial and Medical Ultrasound, Applied Physics Laboratory; and ‡Department of Bioengineering, University of Washington, Seattle, WA, USA; and §Moscow State University, Moscow, Russia

(*Received* 30 *March* 2005, *revised* 31 *May* 2005, *in final form* 7 *June* 2005)

Abstract—An optically transparent phantom was developed for use in high-intensity focused ultrasound (US), or HIFU, dosimetry studies. The phantom is composed of polyacrylamide hydrogel, embedded with bovine serum albumin (BSA) that becomes optically opaque when denatured. Acoustic and optical properties of the phantom were characterized as a function of BSA concentration and temperature. The speed of sound (1544 m/s) and acoustic impedance (1.6 MRayls) were similar to the values in soft tissue. The attenuation coefficient was approximately 8 times lower than that of soft tissues (0.02 Np/cm/MHz for 9% BSA). The nonlinear (B/A) coefficient was similar to the value in water. HIFU lesions were readily seen during formation in the phantom. In US B-mode images, the HIFU lesions were observed as hyperechoic regions only if the cavitation activity was present. The phantom can be used for fast characterization and calibration of US-image guided HIFU devices before animal or clinical studies. (E-mail: vaezy@apl.washington.edu) © **2005 World Federation for Ultrasound in Medicine & Biology.**

Key Words: **Phantom, HIFU, Dosimetry, Ultrasound, Thermal therapy.**

INTRODUCTION

Integration of high-intensity focused ultrasound (US), or HIFU, and an imaging modality is essential for the development of noninvasive therapies that allow accurate targeting and monitoring of lesion formation during hemorrhage control or tumor treatment. A transparent gel phantom was developed that allows HIFU dosimetry and calibration of targeting accuracy of US-image guided HIFU devices, in a fast and controlled manner. A similar phantom was originally developed to investigate thermal coagulation by magnetic resonance-guided microwave ablation (Bouchard and Bronskill 2000).

The gel phantom (polyacrylamide hydrogel embedded with bovine serum albumin, BSA) shows a localized response to HIFU treatment, with a well-defined opaque lesion (produced by BSA protein denaturation) at the HIFU focus. The phantom is transparent, which allows real-time visual observation of lesion formation. The lesions may also be observed as hyperechoic regions in US B-mode images. This phantom has been used extensively for the last 5 years in a number of therapeutic US laboratories. However, few published data exist regarding its properties. We are reporting here on the results of characterization of the acoustic and optical properties of the BSA gel phantom, and the ability to visualize the HIFU-induced gel lesions, both optically and with US B-mode imaging.

Address correspondence to: Shahram Vaezy, Ph.D., Center for Industrial and Medical Ultrasound, Applied Physics Laboratory, 1013 NE 40th Street, Seattle, WA 98105 USA. E-mail: vaezy@apl.washington.edu

MATERIALS AND METHODS

Phantom fabrication

This phantom is based on a polyacrylamide gel mixed with BSA, a protein used as a temperature-sensitive indicator (Bouchard and Bronskill 2000). Polyacrylamide gels are made by a crosslinking copolymerization of acrylamide and N,N′-methylene bisacrylamide (bis) in an aqueous solution (Oppermann et al. 1985). Acrylamide monomer is a neurotoxin and safety precautions (using a fume hood, wearing safety goggles, protective

clothing and gloves) should be taken during the making of the phantom. However, polyacrylamide, a polymerized form of acrylamide, is considered nontoxic (Prokop 2002). The following protocol for phantom fabrication was used: Degassed, distilled water and 1 mol/L TRIS buffer at pH 8 (trizma hydrochloride and trizma base, Sigma Chemical, St Louis, MO, USA) were mixed to dissolve the BSA at concentrations of 3, 5, 7 and 9% (by weight). A 40% w/v acrylamide solution (ICN Biomedicals, Aurora, OH, USA) with a 19:1 ratio of acrylamide:bis in solution was added. The polymerization was initiated by the addition of a 10% (w/v) ammonium persulfate solution (APS, Sigma) and N,N,N′,N′-tetramethylethylene/diamine (TEMED, Sigma) redox system at room temperature. The reaction is slightly exothermic. The resulting mixture consisted of a 7% acrylamide:bis concentration, and 3 to 9% of BSA protein (depending on the experiment). The gels were either tested within 1 h after polymerization or stored in vacuum-sealed, plastic bags to avoid dehydration (if left in air), or swelling (if placed in water).

Characterization of acoustic properties

The acoustic impedance was determined by multiplying the density and the speed of sound of the gel phantom (Christensen 1988). The density of the phantom was determined from the measurements of the mass and volume of the sample using a standard Archimedean technique. The speed of sound (SoS) and attenuation measurements were done using a standard technique with a broadband transmission US system, as described in detail elsewhere (Bloch 1998; Prokop 2002). Briefly, the SoS in the specimen was found by cross-correlation between the sample and reference (pure water path) digitized voltage waveforms. The attenuation coefficient over the 1 to 5 MHz range was obtained using a frequency domain ratio method, in which the logarithm of the spectral magnitude of the signal transmitted through the sample (14 mm thick) is subtracted from the same quantity for the signal transmitted through water for a transducer separation equal to the sample thickness. All measurements were performed at room temperature ($\approx$ 22 °C), with 6 to 8 samples used at each BSA concentration (3, 5, 7 and 9%). The attenuation coefficients at different BSA concentrations were plotted as a function of frequency, and the goodness-of-fit coefficients (R^2) for linear regressions were calculated. In addition, the temperature dependence of the SoS and the attenuation coefficient in the 22 to 82 °C range was determined by immersing 7% BSA gels (three samples) in a thermally regulated water bath. The temperature of the water bath was measured with an alcohol thermometer. The reference SoS in water, as a function of temperature, was calculated (with an error of 0.03 m/s) using the equation established by Marczak (1997).

Characterization of nonlinear acoustic properties

A 48.6-mm diameter piston that operates at a frequency of 720 kHz was used in the experiments for the determination of nonlinearity (B/A) coefficients (Hamilton and Blackstock 1998). The transducer was driven in a pulse regimen as described previously (Birer et al. 2004). The transducer pressure amplitude was adjusted to either 0.05 MPa (for the linear case) or 2 MPa (for the nonlinear case). The pressure measurements were performed in water with a polyvinylidene difluoride (PVDF) hydrophone (Onda Corporation, Sunnyvale, CA, USA) at two distances from the transducer surface (50 and 203 mm). The pressure measurements were also performed at the distance of 203 mm after the US wave propagated through 150-mm long block of the gel (the front face of the gel was 50 mm away from the transducer surface). The SoS in water and in the gel phantom at room temperature was deduced from the measurements in the linear conditions. For the nonlinear case, the absolute pressure was obtained by deconvolution with the impulse response of the hydrophone. The 2-D hydrophone map of the transducer pressure measured at 50 mm was used as an input parameter for the simulation program. The program simulates the propagation of US wave through the 150-mm thick layer of water or BSA gel (concentration of 3 to 9%, room temperature) for different values of B/A. For each simulation, the coefficient of correlation between the theoretical and experimental responses was calculated. The best correlation gave the B/A of the studied media. This method was validated using a reference material, butandiol. Using a known method based on the parametric effects (Barriere and Royer 2001), the B/A of butandiol was found equal to 10.9 $\pm$ 0.5. Our method gave B/A of 11.1 for butandiol, which was in the range given by the reference method. Therefore, our method provided an accurate estimation of the B/A coefficient.

Characterization of optical properties

The index of refraction of the phantom was measured as a function of the BSA concentration. Plastic boxes with transparent and parallel faces were filled with the phantom material and used to measure the optical index of refraction by deflection of a light beam with changing incidence angle. A laser beam illuminated the box at a 90° incidence angle. A rectangular mesh screen was positioned perpendicular to the beam, and a digital picture of the screen was taken to precisely position the initial beam spot. Then, the laser beam incidence angle was set to 45° and the new position of the laser beam was measured. The index of refraction of the plastic was

measured when the box was empty. The index of refraction of the tissue-mimicking material was obtained after successive applications of Snell's law when light was going through air, plastic, the sample, and then again through plastic and air. Four samples were tested at each BSA concentration.

The optical transparency was measured by transmitting a light beam through a thin section of gel, which becomes optically diffusive with thermal denaturation of the BSA indicator protein. The BSA protein denaturation was induced by immersion of the phantom in a thermoregulated transparent water bath. The water bath was filled with distilled degassed water and the water temperature was set between 58 and 66°C. The 7% BSA gel sample was cast inside a thin, waterproof cell (1.6 mm thick, 16 mm in diameter). The body of the cell was constructed of copper plate with the cell walls made of thin glass plates (0.17-mm microscope slide covers) to allow light transmission. The gel mixture was introduced into the cell with hypodermic needle through small holes drilled in the edge of the copper plate and allowed to polymerize. The white light source was collimated into a beam using a pinhole and lens and an iris was used to adjust the beam diameter (of 6 mm). A beam splitter was used to transmit half of the light through the water bath and the sample and the other half of the light was directed to a photodiode to monitor any change in the light intensity related to the source. The direct current (DC) electric voltage produced by the photodiode circuits were recorded as a function of time using a 12-bit digitizer and a Labview interface (National Instruments, Austin, TX, USA). The ratio between the two photodiode voltages represented the degree of opacity of the sample.

HIFU lesion production in the gel phantom

HIFU lesions were produced in a gel phantom with 7% BSA concentration. The HIFU transducer was a single-element concave transducer with a center frequency of 3.5 MHz, diameter of 33 mm and radius of curvature of 35 mm (Sonic Concepts, Woodinville, WA, USA). The acoustic power of the transducer was measured using absorptive radiation force balance (Christensen 1988). In this method, the incident US energy striking an absorptive target causes a transfer of momentum to that target, manifested as measurable force that can be converted into acoustic power. Acoustic powers, used in our experiments, were measured to be in the range of 8 to 23 W. The mapping of US field of the HIFU transducer was performed using a needle hydrophone (TNU001A, NTR Systems, Seattle, WA, USA). A custom-made Labview program was used to control the stepper motor that was moving the hydrophone and to collect and plot the signal from the hydrophone. The focal beam width and length, obtained from the −3-dB contour of the transducer pressure amplitude, were measured to be 0.45 mm and 4.1 mm, respectively. The cross-sectional focal area was 0.16 mm^2. US intensities were obtained by dividing the acoustic power with the focal area, and then derated with tissue or gel attenuation to obtain *in situ* intensities (Christensen 1988). The HIFU exposure durations were 3, 5 and 7 s. The HIFU dose at the focal area was calculated as the *in situ* intensity at the focus (spatial-average, temporal-average) multiplied by the exposure duration, resulting in units of J/cm^2.

The US imaging probe (CL10-5, HDI 1000, Philips, Bothell, WA, USA) and HIFU transducer were rigidly clamped in an assembly so that the acoustic axis of the HIFU beam coincided with the imaging plane. The protocol of real-time visualization of US-guided HIFU treatment is described in detail elsewhere (Vaezy et al. 2001). The direct visualization of the HIFU focal region was achieved using a digital camcorder with a + 4 diopter close-up lens (Quantaray, Beltsville, MD, USA). Video footages of lesions observed visually and with US imaging were digitized and edited on a video-processing workstation (Premiere 6.0, Adobe, San Jose, CA, USA). The images of the lesions were traced by the same operator in ImageJ using a graphics tablet (Graphire2, Wacom Technology, Vancouver, WA, USA), and the lesion volumes were then calculated using a custom-made Matlab program. Lesions were assumed to be axially symmetrical.

RESULTS

The SoS and density at room temperature were found to be independent of BSA concentration in the range of 3 to 9%. The SoS was 1544 ± 11 m/s (mean ± SD), and the density was 1044 ± 15 kg/m^3. These results yielded an acoustic impedance of 1.6 MRayls.

The attenuation coefficient was approximately linear over the 1- to 5-MHz frequency range (Fig. 1), with the coefficients of 0.009 (R^2 = 0.93), 0.013 (R^2 = 0.98), 0.017 (R^2 = 0.99) and 0.021 (R^2 = 0.98) Np/cm/MHz

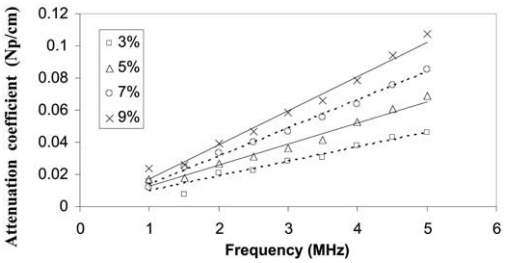

Fig. 1. Attenuation coefficient as a function of BSA concentration and frequency. The data points represent an average of 6 to 8 measurements.

measured for BSA concentrations of 3, 5, 7 and 9%, respectively. The attenuation increased linearly with the increase in the BSA concentration. The attenuation coefficient of the phantom was approximately 8 times lower (for 9% BSA concentration) than that for the soft tissues. The SoS was found to be temperature-dependent, with a maximum of 1590 m/s near 60 °C (Fig. 2a). The attenuation coefficient showed an opposite trend with a minimum near 50 °C (Fig. 2b).

The values of the nonlinearity coefficient B/A at room temperature are provided in Table 1. The B/A of the gel phantom was similar to the B/A of water. No significant variation of B/A was observed with the change in the BSA concentration in 3 to 9% range. Based on the SD of the measured B/A values for water, the estimate of the method precision is ± 3%.

BSA (3 to 9%) and acrylamide (7%) concentrations produced an optically clear amber-colored gel, because the exothermic polymerization reaction was not energetic enough to denature the embedded BSA protein. The index of refraction of the phantom was 1.29 ± 0.02 (mean ± SD). No statistically significant difference was found between indices of refraction for specimens of different BSA concentrations. Figure 3 shows optical transmission of a 7% BSA gel phantom as a function of temperature (in 58 to 66 °C range) and thermal exposure time. The gel opacity increased (*i.e.*, the optical transmission decreased) with the increase in gel temperature

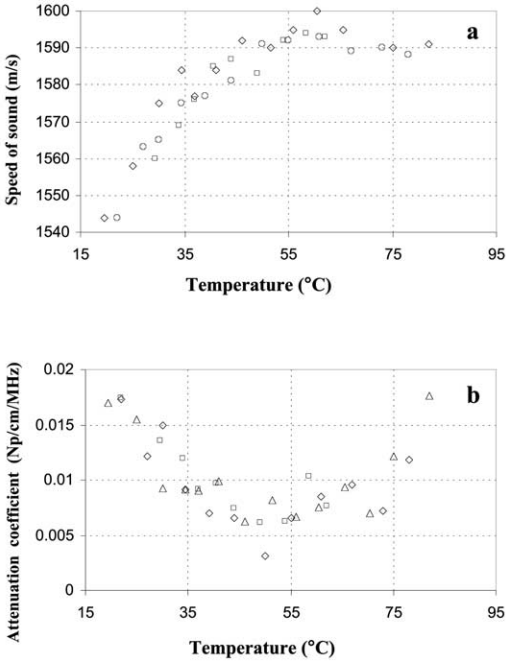

Fig. 2. Temperature-dependence of (a) the speed of sound and (b) attenuation coefficient for 7% BSA concentration.

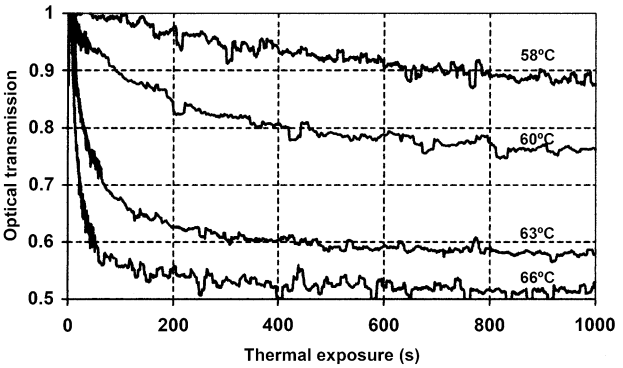

Fig. 3. Light transmission through 7% BSA gel phantom as a function of temperature and the duration of thermal exposure.

and/or longer duration of the gel exposure to the elevated temperature.

The gel phantom allowed easy observation of the HIFU lesion formation, noted as a significant increase in the gel opacity. The lesions appeared to form either because of purely thermal effects (*i.e.*, a gradual heating resulting in well-defined cigar-shaped lesions) (Fig. 4a), or because of a combination of thermal and cavitational effects (*i.e.*, bubble formation and apparent boiling) resulting in tadpole-shaped (Fig. 4b)) or egg-shaped lesions (Fig. 4c)) with coarse boundaries. It was possible to optically visualize the cavitation activity inside the lesions when it occurred. With US B-mode imaging, the HIFU lesions were observed as a hyperechoic region only if the cavitation activity was present (in 89% of the HIFU exposures). No US visualization of purely thermal lesions was achieved (Fig. 4a). Figure 5 shows US image-based lesion volumes vs. optical lesion volumes. In general, lesions appeared bigger in US images, as compared to their actual size.

The optical volume of the HIFU lesions produced in 6% BSA gel phantom is plotted in Fig. 6 as a function of HIFU dose (*in situ* intensity*HIFU exposure duration) and compared with corresponding lesions produced in turkey breast *in vitro*. At the same HIFU dose, the gel lesions were substantially smaller as compared to tissue lesions.

DISCUSSION

We have measured acoustic and optical properties of the gel phantom used in HIFU dosimetry studies. The SoS and acoustic impedance were similar to the values in soft tissue, and nonlinearity coefficient was similar to the values in water. The attenuation coefficient was approximately an order of magnitude lower as compared to soft tissues. Both thermal and cavitational HIFU lesions in the phantom were readily seen under optical visualiza-

Table 1. Nonlinearity parameter (B/A) of the gel phantom at room temperature as a function of the BSA concentration

[BSA] %	0	3	5	7	9
B/A gel	4.8	5.1	4.8	5	5
B/A water	4.9	4.8	4.6	4.9	4.9

tion, but only cavitational lesions could be visualized with US B-mode imaging.

The acoustic attenuation of the phantom was substantially lower than that of tissues. For example, at 3 MHz the attenuation coefficient of 9% BSA gel was 0.06 Np/cm, which is 7.5 times lower than the attenuation coefficient of the liver and striated muscle at the same frequency (Christensen 1988). This resulted in the lesion volumes in BSA gel phantom being an order of magnitude smaller as compared to the lesions in tissue (turkey breast) at the same HIFU dose. The attenuation coefficient and SoS were dependent on temperature in our experiments, which was in accordance with previously reported results (Damianou et al. 1997; Techavipoo et al. 2002).

The nonlinear properties of biologic tissues induce distortion of US waves when high pressures are involved. Knowing the parameter of nonlinearity B/A of the gel phantom seemed of major importance to us because HIFU produces such exposure conditions. Our proposed method for measuring B/A was based on the comparison between theoretical simulations and experimental results. The theoretical model allows the simulation of the propagation (time domain) of an US plane wave in successive nonlinear, attenuating and dissipative media. The B/A coefficient was practically the same for the BSA gel and water, which is not surprising because the gel is mostly composed of water (≈ 70%).

No thermal properties of the BSA gel phantom are reported here. However, the BSA phantom is expected to have similar properties to the egg-white polyacrylamide gel phantom (with egg-white as an indicator protein instead of BSA), that was shown previously to have specific heat (Cp) of 4270 ± 365 J/Kg/ °C and thermal conductivity (k) of 0.59 ± 0.06 W/m/ °C (Divkovic and Jenne 2004). These values are very similar to the values of water (which has Cp of 4185 J/Kg/ °C and k of 0.60 W/m/ °C). The BSA gel phantom denatured at the temperatures in excess of 58 °C, which agreed well with the previously reported results (Bouchard and Bronskill 2000).

The calibration of diagnostic US imaging devices has been performed previously with water-based gel phantoms embedded with powdered graphite or glass beads that cause US backscattering (Madsen et al. 1991). Castor oil, with an attenuation coefficient of 0.95 dB/cm at 1 MHz (Wells 1969), is useful in the estimation of pressure fields in soft tissue. Granz (1994) proposed 1,3 butanediol for high-amplitude applications because this material mimics tissue in US speed, impedance, absorption, nonlinearity parameters and reaction to acoustic cavitation. Solid phantoms, such as graphite powder embedded in agar gel (Holt and Roy 2001), have been used to produce a medium for which acoustical and thermal features are similar to those of tissues. Phantoms, consisting of closely packed agar spheres (0.3 to 3.6 mm in diameter) surrounded with 10% propanol solution, have also been developed for calibration of US hyperthermia systems (Chin et al. 1990). However, none of these phantoms was suitable for the calibration and dosimetry

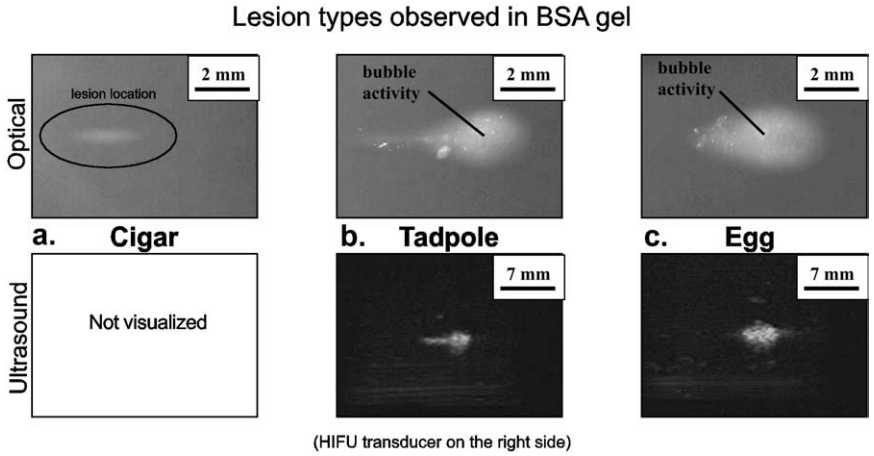

Fig. 4. Lesions formed in 6% BSA gel phantom and the corresponding US images (if visualization occurred). (a) Cigar-shaped lesion, (b) tadpole-shaped lesion, and (c) egg-shaped lesion. Note that the scale bar in US images is 3.5 times larger as compared to the scale bar in gross images.

of HIFU devices. Disadvantages of these previous phantoms include US-induced streaming (liquid phantoms), phantom melting (agar phantoms), lack of optical transparency (tissue and graphite-based phantoms) and lack of thermal lesion formation.

Current methods of guiding and monitoring HIFU applications for noninvasive therapies include magnetic resonance imaging and diagnostic US imaging techniques (Hynynen et al. 2001; Wu et al. 2001). Magnetic resonance imaging and computer tomography can be used to quantify the lesion formation and temperature elevation in usually opaque tissue samples and phantoms. However, for optimization of US image-guidance of HIFU treatment, a phantom development was needed that would allow real-time monitoring of the lesion formation, both optically and with B-mode US imaging. The transparent nature of the BSA gel phantom for the selected range of BSA concentrations permits real-time observation of HIFU-induced lesions.

In contrast to the turkey breast, in which inhomogeneties may have interfered with the HIFU delivery, the BSA gel phantom is more homogeneous. The stock BSA protein is a fine powder and is expected to be evenly suspended within the polyacrylamide polymer. The relative homogeneity of the gel phantom is apparent when comparing the linearity of the optical lesion volumes vs. dose for the gel phantoms as compared to the turkey breasts (Fig. 6). Turkey breast may be a better model of a clinical treatment caused by the natural inhomogeneity inherent in tissue that may complicate targeting and formation of lesions. However, for the purposes of studying the effects of HIFU and comparing to theoretical simulations that assume homogeneous materials, the homogeneity of the gel phantom is preferred.

The use of US visualization for the guidance and monitoring of HIFU therapies most often relies on the appearance of a hyperechoic region in the US image

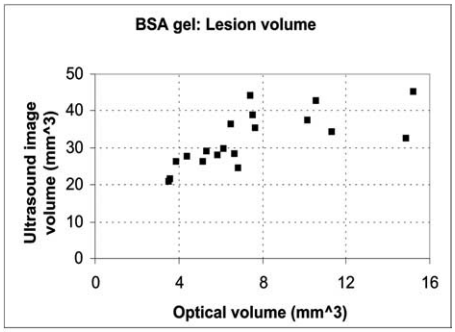

Fig. 5. Optical lesion volume vs. lesion volume estimated from US images.

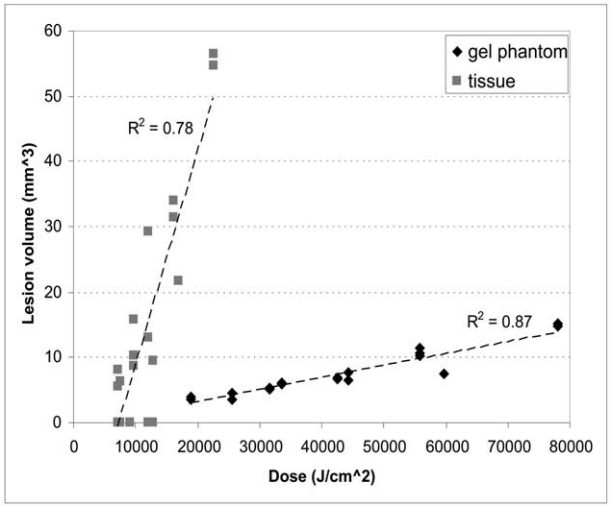

Fig. 6. Lesion volume vs. HIFU dose for BSA gel phantom and tissue (turkey breast *in vitro*).

(ter Haar et al. 1989; Wu et al. 2001). Based upon our observations of the HIFU exposures in the gel phantom, optically observed bubble activity coincided with US B-mode visualization of the lesion formation, in the form of a hyperechoic region. Previous work suggests that the hyperechoic regions are caused by the formation of gas bubbles at the focus of the HIFU beam (Bailey et al. 2001). Lesions that were visualized using US imaging typically had tadpole- or egg-shaped optical geometries. In the gel phantoms, there appeared to be a resemblance in the optical lesion geometry and the corresponding hyperechoic region observed on the US B-mode images. Thermal effects of HIFU were visualized optically as cigar-shaped lesions. Thermally generated lesions were not visualized *via* US B-mode imaging, probably because of the lack of bubble activity within this lesion type.

In summary, the BSA gel phantom has advantages of the ease of manufacturing and use, relatively low cost and localized denaturation in response to HIFU energy that can be observed both visually and with US imaging. This phantom is becoming a necessary everyday tool in therapeutic US laboratories for calibration and performance testing of different HIFU devices before *in vivo* experiments. We believe that this phantom will be equally useful for device calibration in future clinical studies.

Acknowledgements—The authors acknowledge support from DARPA (no. N00014-96-1-0630), the US NIH (no. HL64208-02), NSF (BES-0002932) and NSBRI (no. PF00505). We thank John I. Clark for his advice on making a gel with the desired optical property of phase transition at HIFU intensities.

REFERENCES

Bailey MR, Couret LN, Sapozhnikov OA, et al. Use of overpressure to assess the role of bubbles in focused ultrasound lesion shape *in vitro*. Ultrasound Med Biol 2001;27:695–708.

Barriere C, Royer R. Diffraction effects in the parametric interaction of acoustic waves: Application to nonlinearity parameter measurements in liquids. IEEE Trans Ultrason Ferroelec Freq Control 2001;48:1706–1715.

Birer A, Ghohestani M, Cathignol D. Generation of higher pressure pulses at the surface of piezo-composite materials using electrical pre-strain. IEEE Trans Ultrason Ferroelec Freq Control 2004;51: 879–886.

Bloch S. Ultrasonic tissue characterization: towards high-intensity focused ultrasound treatment monitoring. MA thesis. Department of Bioengineering, University of Washington, 1998.

Bouchard LS, Bronskill MJ. Magnetic resonance imaging of thermal coagulation effects in a phantom for calibrating thermal therapy devices. Med Phys 2000;27:1141–1145.

Chin RB, Madsen EL, Zagzebski JA, et al. A reusable perfusion supporting tissue-mimicking material for ultrasound hyperthermia phantoms 1990;17:380–390.

Christensen DA. Ultrasonic bioinstrumentation. New York: John Wiley and Sons, 1988.

Damianou CA, Sanghvi NT, Fry FJ, Maas-Moreno R. Dependence of ultrasonic attenuation and absorption in dog soft tissues on temperature and thermal dose. J Acoust Soc Am 1997;102:628–634.

Divkovic G, Jenne JW. Phantome für die Therapie mit hochenergetischem fokussiertem Ultraschall. Ultraschall Med 2004;25:15.

Granz B. Measurement of shock wave properties after the passage through a tissue mimicking material. IEEE Trans Ultrason Ferroelec Freq Control Sympos Proc 1994;3:1847–1851.

Hamilton MF, Blackstock DT. Nonlinear acoustics. San Diego, CA: Academic Press. 1998.

Hynynen K, Pomeroy O, Smith DN, et al. MR imaging-guided focused ultrasound surgery of fibroadenomas in the breast: A feasibility study. Radiology 2001;219:176–185.

Holt RG, Roy RA. Measurements of bubble-enhanced heating from focused, MHz-frequency ultrasound in tissue-mimicking material. Ultrasound Med Biol 2001;27:1399–1412.

Madsen EL, Zagzebski JA, Macdonald MC, Frank JR. Ultrasound focal lesion detectibility phantoms. Med Phys 1991;18:1171–1180.

Marczak W. Water as a standard in the measurements of speed of sound in liquids. J Acoust Soc Am 1997;102:2776–2779.

Oppermann W, Sigrid R, Rehage G. The elastic behavior of hydrogels. Br Polymer J 1985;17:175–180.

Prokop AF. Polyacrylamide gel as an acoustic coupling medium for therapy applications of high intensity focused ultrasound. Bioengineering, University of Washington, 2002.

Techavipoo U, Varghese T, Zagzebski JA, Stiles T, Frank G. Temperature dependence of ultrasonic propagation speed and attenuation in canine tissue. Ultrason Imaging 2002;24:246–260.

ter Haar G, Sinnett D, Rivens I. High intensity focused ultrasound—A surgical technique for the treatment of discrete liver tumours. Phys Med Biol 1989;34:1743–1750.

Vaezy S, Shi X, Martin RW, et al. Real-time visualization of high-intensity focused ultrasound treatment using ultrasound imaging. Ultrasound Med Biol 2001;27:33–42.

Wells PNT. Physical principles of ultrasonic diagnosis. New York: Academic Press, 1969.

Wu F, Chen W, Bai J, et al. Pathological changes in human malignant carcinoma treated with high-intensity focused ultrasound. Ultrasound Med Biol 2001;27:1099–1106.